Weierstraß-Institut

für Angewandte Analysis und Stochastik

im Forschungsverbund Berlin e. V.

Preprint ISSN 0946 – 8633

Saturation of the all-optical Kerr effect

Carsten Brée[1,2], Ayhan Demircan[1], Günter Steinmeyer[2,3]

submitted: September 24, 2010

[1] Weierstrass Institute for Applied Analysis and Stochastics, Mohrenstraße 39, 10117 Berlin, Germany

[2] Max Born Institute for Nonlinear Optics and Short Pulse Spectroscopy, Max-Born-Straße 2A, 12489 Berlin, Germany

[3] Optoelectronics Research Centre, Tampere University of Technology, 33101 Tampere, Finland

No. 1540

Berlin 2010

2010 *Mathematics Subject Classification.* Primary 78A60.

2008 *Physics and Astronomy Classification Scheme.* 42.65.Tg, 42.65.-k,52.38.Hb,42.68.Ay.

Key words and phrases. Nonlinear Optics, all-optical Kerr effect, Femtosecond Filamentation.

We kindfully acknowledge financial support by the Deutsche Forschungsgemeinschaft, grants DE 1209/1-2 and STE 762/7-2.

Edited by
Weierstraß-Institut für Angewandte Analysis und Stochastik (WIAS)
Mohrenstraße 39
10117 Berlin
Germany

Fax: +49 30 2044975
E-Mail: preprint@wias-berlin.de
World Wide Web: http://www.wias-berlin.de/

Abstract

Saturation of the intensity dependence of the refractive index is directly computed from ionization rates via a Kramers-Kronig transform. The linear intensity dependence and its dispersion are found in excellent agreement with complete quantum mechanical orbital computations. Higher-order terms concur with solutions of the time-dependent Schrödinger equation. Expanding the formalism to all orders up to the ionization potential of the atom, we derive a model for saturation of the Kerr effect. This model widely confirms recently published and controversially discussed experimental data and corroborates the importance of higher-order Kerr terms for filamentation.

Most nonlinear optical effects can be understood in the perturbative limit with two or three interacting optical waves, giving rise to contributions $\chi^{(2)}_{ij}E_iE_j$ or $\chi^{(3)}_{ijk}E_iE_jE_k$ to the polarization P, respectively. Higher-order $\chi^{(n)}(n \geq 4)$ terms can be formally considered. Yet, a perturbative description of higher order effects is rarely useful as often enough a large number of waves interact simultaneously as, for example, in high-harmonic generation [1]. The role of $\chi^{(5)}$ effects for arresting catastrophic optical self-focusing has been discussed already more than 20 years ago [2, 3, 4]. $\chi^{(3)}$ effects, namely the all-optical Kerr effect, give rise to an increase of the refractive index with intensity $n = n_0 + n_2 I$ and a resulting focusing nonlinear lens. A $\chi^{(5)}$ dependence with negative sign and defocusing nonlinear lensing would explain the phenomenon of filamentation, i.e., the formation of long self-guided light strings with nearly constant diameter. Early experimental results indicated that filamentation cannot only be explained by plasma formation [5], which gives rise to a negative index contribution suitably described by Drude theory. Nevertheless, refined theoretical models succeeded in explaining even complex experimental results without the need for including a saturation of the Kerr effect [6, 7]. Recently, this accepted picture was challenged by measurements [8, 9] that indicate yet again a strong influence of higher-order nonlinearities to the extent that filament formation is explained in the complete absence of plasma formation. These results have been controversially discussed [10]. In the following, we provide an independent and previously unreported approach towards computing Kerr saturation. Our approach is based on a Kramers-Kronig transform [11] of optical absorption derived from Keldysh theory [12]. This analysis supports the experimental results in Ref. [8], indicating that we may have in fact a paradigm shift in explaining femtosecond filamentation [10].

Our model is based on a recent modification [12] of Perelomov-Popov-Terent'ev (PPT) theory [13], the former providing cross-sections for multiphoton ionization according

to

$$\sigma_K(\omega) = \frac{2\sqrt{2}C^2}{\pi}(2e)^{2n^*}\left(\frac{e}{2}\right)^{2K}\omega_{\rm p}^{-3K+1}\left(\frac{q_{\rm e}^2}{\hbar m_{\rm e}\varepsilon_0 c}\right)^K\left(\frac{\omega_{\rm p}}{\omega}\right)^{2n^*+2K-3/2} \times \exp\left(-\frac{\omega_{\rm p}}{\omega}\right) w_0\left[\sqrt{2K-2\frac{\omega_{\rm p}}{\omega}}\right] \quad (1)$$

for $\omega \geq \omega_{\rm p}/K$. Here ω is the optical frequency, $q_{\rm e}$ and $m_{\rm e}$ denote electron charge and mass, respectively, ε_0 is the vacuum dielectric constant, and c denotes vacuum light speed. $\hbar\omega_{\rm p}$ is the ionization potential of the gas species under consideration. The constant $K = \langle \omega_{\rm p}/\omega + 1\rangle$ counts the number of photons required for ionization, where $\langle x\rangle$ denotes the integer part of x. The effective prinicipal quantum number of the bound state is given by $n^* = Z\sqrt{\omega_{\rm H}/\omega_{\rm p}}$, where $\hbar\omega_{\rm H} = 13.6\,$eV is the Rydberg energy. The constant $C = 2^{n^*-1}/\Gamma(n^*+1)$ is related to the asymptotic expansion of the ground-state electronic wavefunction, and $w_0[x]$ denotes Dawson's function [14]. From the cross-sections σ_K, the K-photon absorption coefficients $\Delta\alpha_K$ may then be calculated according to

$$\Delta\alpha_K(\omega) = K\hbar\omega\rho_{\rm nt}\sigma_K I^{K-1}, \quad (2)$$

with a particle density $\rho_{\rm nt} = 2.7\times10^{19}{\rm cm}^{-3}$ corresponding to standard conditions. For atomic argon, this perturbative approximation is expected to hold for intensities up to $50\,{\rm TW/cm}^2$, i.e., well within the intensity limits considered below.

Kramers-Kronig theories have been successfully applied to nonlinear refraction in solids [11, 15]. Here we combine this method with Keldysh theorey to compute nonlinear refraction in inert gases. In principle, as pointed out in [11], the use of Kramers-Kronig relations requires knowledge of nondegenerate multiphoton absorption coefficients $\Delta\alpha_K^N(\omega_1,...,\omega_K)$. These coefficients cannot easily be provided by PPT theory. Instead, we use

$$\Delta\alpha_K^N(\omega_1,\omega_2,....,\omega_K) = \Delta\alpha_K(\frac{\omega_1+...+\omega_K}{K}), \quad (3)$$

as an estimate, generalizing the model successfully used to compute n_2 in solids [15]. Using this proven simplification, we find that the nonlinear refraction coefficients n_{2k} are related to $(k+1)$-photon absorption coefficients σ_{k+1} via the KK relations according to

$$n_{2k}(\omega) = \frac{\hbar c\rho_{\rm nt}}{\pi}\fint_0^\infty(\Omega+k\omega)\frac{\sigma_{k+1}\left(\frac{\Omega+k\omega}{k+1}\right)}{\Omega^2-\omega^2}d\Omega, \quad (4)$$

where $\fint$ denotes Cauchy's principal value integral. As an example, setting $k=1$, we calculate the leading term $n_2(\omega)$ of nonlinear refraction for helium [Fig. 1]. Among the inert gases, helium is the least complex atom and the only one for which detailed computations of n_2 from atomic wave functions exist. For large wavelengths, our analysis indicates a value $n_2 = 4.8\times10^{-9}\,{\rm cm}^2/{\rm TW}$, which deviates by only 26% from the value $3.8\times10^{-9}\,{\rm cm}^2/{\rm TW}$ that was derived by Bishop and Pipin using explicitly electron-correlated wave functions [16]. Keeping in mind that the absorption spectra σ_K have

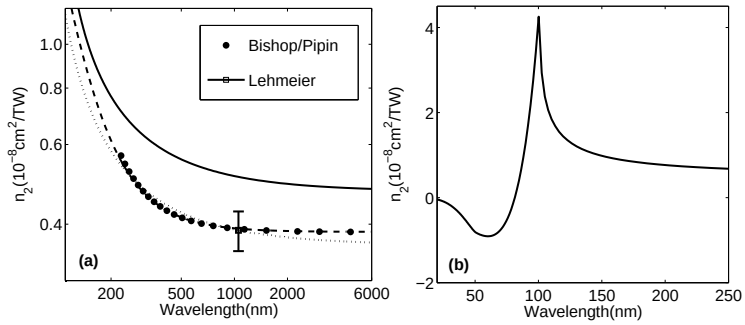

Figure 1: (a) Nonlinear refractive index n_2 of He below the 2PA resonance at $\lambda = 85$ nm. Solid lines: n_2 dispersion as extracted from Eq. (4). Dashed line: fit of theoretical data to scaling law (dots) from [19]. (b) Same in the vicinity of the resonance.

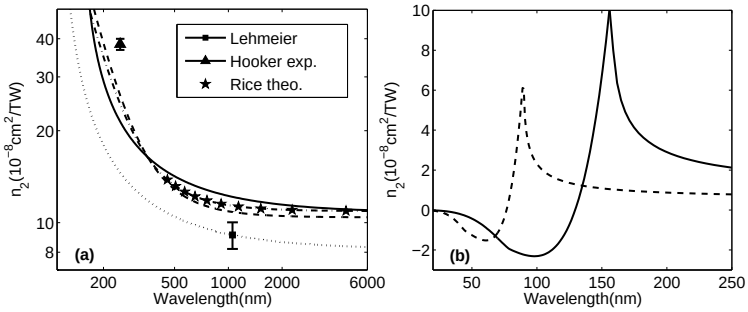

Figure 2: (a) Nonlinear refractive index n_2 of Ar from Eq. (4) below the 2PA resonance. Dash-dotted line: power series in ω^2 [19, 20] fitted to theoretical data [20] (stars). Dashed line: experimental n_2 data [19] Dotted line: Lehmeier data extrapolated with scaling law given in [17]. (b) n_2 of neutral argon in the vicinity of the 2PA resonance at $\lambda = 85$ nm [solid line, Eq. (4)]. Dashed line: n_2 of singly ionized Ar^+.

been derived from strong field ionization rates for which often an order of magnitude agreement with experimental data is considered reasonable, our Kramers-Kronig approach provides an excellent prediction of n_2. Our model also correctly reproduces the dispersive behavior of n_2 predicted in Ref. [16] and reasonably agrees with experimental data at $1.06\,\mu$m wavelength [17]. Even better agreement is obtained for argon [Fig. 2]. Going beyond the tabulated values of [16] for helium, our computations predict that n_2 reaches a maximum value $n_2 \approx 4 \times 10^{-8}$ cm^2/TW at about 100 nm wavelength, which corresponds to half the ionization energy. Going to even smaller wavelengths, n_2 crosses zero at 85 nm and stays negative up to the ionization energy equivalent of 50.4 nm wavelength. This prototypical behavior with a sign change at approximately 60% of the ionization threshold is seen for all inert gases and duplicates the dispersion characteristics of n_2 in solids [15]. Compared to our previous work [18], the possibility to extend n_2 computation beyond half the ionization energy into the negative region

and the correct prediction of its dispersion in the positive region both arise from usage of the improved ionization cross sections provided in Ref. [12].

Similarly good agreement of Eq. (4) with independent experimental and theoretical data is obtained for neon, krypton and xenon, for which our approach reproduces experimental and theoretical data [19, 20] within 15% precision.

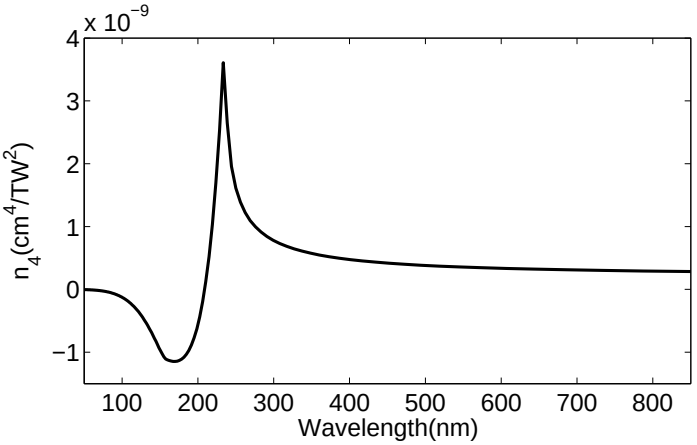

Figure 3: (a) Dispersion of n_4 [Eq. (4) with $k = 2$] in the vicinity of the 3PA absorption edge at $\lambda = 236$ nm.

Figure 2 shows an n_2 computation for argon showing similar features as the helium example. Given that the ionization energy of argon is only 15.76 eV and that a smaller number of photons is required to reach the continuum, n_2 of argon is about a factor of 20 larger in the infrared, with a value of $\approx 10^{-7}$ cm^2/TW. This value agrees favorably with commonly used reference data [17] and was also reproduced by Loriot *et al.* in their measurements. Compared to helium, the zero crossing of n_2 is now shifted to a wavelength of 140 nm.

$n_2(10^{-8}\frac{\text{cm}^2}{\text{TW}})$	$Z=1$	$Z=2$	$n_2(\omega \to 0)$	Refs.[19, 16]
He	0.52	0.03	0.48	0.38
Ne	1.31	0.27	1.18	0.96
Ar	12.68	6.14	10.84	10.40
Kr	30.69	17.28	25.63	23.17
Xe	91.58	55.17	73.87	61.39

Table 1: Nonlinear refractive index n_2 at 800 nm for Ar and Ar$^+$ ($Z = 1$), ($Z = 2$) and Ar in the static limit $n_2(\omega \to 0)$. Experimental data (rightmost column) as compiled from [19, 16] and corrected for the dispersion of the DFWM process with Eq. (13) in [18].

Nonlinear refraction, in principle, holds two potential mechanisms for saturation. First, the generation of free electrons will replace a number of neutral atoms by ions. In the case of Ar$^+$, this raises the ionization threshold to 27.63 eV, which, in turn, has to

reduce the resulting n_2 values as illustrated by the transition from argon to helium. A computation of the resulting values for Ar^+ is shown as the dashed line in Fig. 2(b), which confirms a reduction of n_2 by a factor of ≈ 2. Table 1 lists computed values of n_2 of all noble gases and their first ionic species ($Z = 1, 2$) for 800 nm wavelength.

While this first mechanism suggests a depletion of the neutral atoms as the cause for saturation, the same effect may also occur due to higher-order Kerr terms n_{2k} with $k \geq 2$. These terms can also be computed using our theoretical approach. As an example, we have plotted $n_4(\omega)$ in Fig. 3. According to our model, argon displays an infrared limit $n_4(\omega \to 0) = 2 \times 10^{-10}\,\mathrm{cm}^4/\mathrm{TW}^2$, reaches a 12 times higher maximum value at 240 nm, and is negative below 210 nm. This behavior is again in agreement with the prototypical dispersion of the Kerr coefficients, yet caused by three-photon rather than two-photon absorption. There is an apparent contradiction to the negative value $n_4 = -0.36 \pm 1.03 \times 10^{-9}\,\mathrm{cm}^4/\mathrm{TW}^2$ reported in Ref. [8]. In principle, a negative n_4 value at 800 nm appears to be incompatible with the dispersion of the Kerr terms predicted by our model.

k	Helium	Neon	Argon	Krypton	Xenon
1	5.21e-09	1.31e-08	1.27e-07	3.07e-07	9.16e-07
2	2.41e-12	9.64e-12	2.90e-10	1.09e-09	5.63e-09
3	2.48e-15	1.56e-14	1.42e-12	8.26e-12	7.32e-11
4	4.54e-18	4.47e-17	1.23e-14	1.11e-13	1.73e-12
5	1.31e-20	2.03e-19	1.72e-16	2.46e-15	7.05e-14
6	5.54e-23	1.34e-21	3.64e-18	8.63e-17	5.39e-15
7	3.24e-25	1.23e-23	1.16e-19	5.16e-18	7.21e-16
8	2.52e-27	1.56e-25	5.92e-21	1.36e-18	-4.78e-17
9	2.56e-29	2.59e-27	7.82e-22	-4.28e-20	-6.82e-19
10	3.33e-31	5.80e-29	-3.78e-23	-6.14e-22	-1.02e-20
11	5.58e-33	1.76e-30	-5.98e-25	-7.64e-24	-1.72e-22
12	1.19e-34	8.01e-32	-6.41e-27	-1.08e-25	-3.04e-24
13	3.34e-36	1.24e-32	-7.85e-29	-1.63e-27	-5.51e-26
14	1.49e-37	-2.34e-34	-1.04e-30	-2.53e-29	-1.01e-27
15	1.37e-38	-1.82e-36	-1.42e-32	-3.98e-31	-1.87e-29
16	-2.95e-40	-1.44e-38	-1.97e-34	-6.33e-33	-3.45e-31

Table 2: Nonlinear refraction coefficients $n_{2k}(\mathrm{cm}^{2k}/\mathrm{TW}^k)$ for the inert gases at 800 nm. n_{2k} relates to the cross-section σ_{k+1} of $k+1$-photon absorption via Kramers-Kronig theory.

The analysis of higher-order Kerr terms can easily be continued to arbitrary order k in our model, even beyond the highest-order experimental n_{10} term in Ref. [8]. For argon at a wavelength of 800 nm, our computation predicts positive coefficients up to n_{18} and negative ones for all higher-order terms. Positive nonlinear refraction up to a 10-photon effect appears to be in strong contrast to the alternating sequence of coefficients measured by Loriot *et al.* A compilation of our computed coefficients is listed in Table 2. Despite the different structure of this saturation mechanism, our computed

coefficients [Fig. 4(a)] show a good qualitative agreement of the nonlinearly-induced index change $\Delta n_{\mathrm{Kerr}} = n_2 I + n_4 I^2 + n_6 I^3 + ...$ with the experimental results for argon in [8]. Our model predicts an increase of Δn_{Kerr} up to about 42 TW/cm^2 and inversion of the index change at 49 TW/cm^2. This is contrasted by experimental values of 30 TW/cm^2 and 34 TW/cm^2, respectively. Apart from this apparent scaling issue, both curves agree remarkably well. In fact, taking into account experimental error estimates of [8], our results turn out to be compatible with the experimentally measured curves. For He, Ne, Kr and Xe, from the coefficients shown in table (2), we deduce inversion intensities of 112, 89, 40, and 30 TW$/$cm^2, respectively. Our analysis also qualitatively agrees with solutions of the time-dependent Schrödinger Equation for atomic hydrogen [21], which, however, indicate saturation at higher values. Despite of delivering higher inversion intensity than reported in [8], our model nevertheless confirms plasma clamping to occur at significantly higher intensities than Kerr saturation. Figure 4(a) shows the refractive index change $\Delta n(I) = n_2 I - \rho/2\rho_{\mathrm{c}}$ induced by the generation of free electrons with density ρ under experimental conditions of [8]. $\rho_{\mathrm{c}} = m_{\mathrm{e}}\varepsilon_0\omega^2/q_{\mathrm{e}}^2$ is the critical plasma density. Clearly, plasma clamping is expected at intensities beyond ≈ 100 TW/cm^2, i.e., well above Kerr saturation.

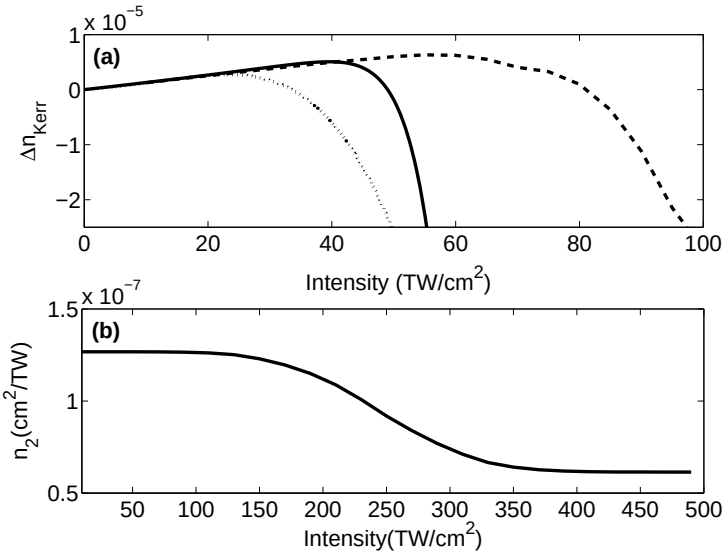

Figure 4: (a) Kerr saturation in argon at 800 nm due to higher order Kerr terms [Eq. (4), solid line], classical filamentation model due to plasma clamping (dashed line), and experimental results [8]
(dotted line). (b) Computed reduction of n_2 resulting from depletion of neutral atoms.

In a second simulation, we model the potential effect of depletion of neutral atoms on the index change. Given a fraction p of ionized atoms, we compute

$$n_2(I) = p n_{2,\mathrm{Ar}^+} + (1-p) n_{2,\mathrm{Ar}}, \tag{5}$$

where p is computed under the assumption of 90 fs Gaussian pulses using the ionization model of [12], duplicating experimental conditions of Ref. [8]. In this case we also

yield a saturation behavior, yet at much higher intensities [Fig. 4(b)]. Complete ionization of argon requires intensities of $\sim 300\,\mathrm{TW/cm^2}$, and even then only a 50% index change results. As this happens nearly an order of magnitude beyond the inversion intensities discussed previously, depletion effects can be clearly ruled out.

These results shed new light on the long-disputed mechanism behind filament formation. First and foremost, saturation of the Kerr effect cannot be explained by inclusion of the next higher-order coefficient n_4 alone. Instead, similar as in the transition from third-harmonic generation to high-harmonic generation, many coefficients start to act simultaneously, and the perturbative description of the effects becomes impractical. While a true depletion-caused saturation $n_2(I) = n_2(0)/(1 + I/I_{\mathrm{sat}})$ can be developed into a Taylor series in I resulting in a sequence of n_{2k} with alternating signs, our model predicts that all n_{2k} are positive until the driving $(k+1)$-photon process reaches about 75% the ionization energy. This causes a nearly unperturbed linear increase of the index change Δn_{Kerr} up to a certain threshold. Above this threshold, Δn_{Kerr} will rapidly decrease and reach strong negative values. Comparing the absolute values of n_4 from our model with Ref. [8], we generally compute smaller values than found in Taylor series analysis of experimental data. This finding corroborates that saturation of the Kerr effect may be perfectly compatible with experimentally observed efficiencies of fifth-order harmonic generation processes [10].

Despite its slightly different functional shape, our results qualitatively confirm the saturation behavior suggested by Loriot *et al.*. This agreement strongly suggests to include a saturation mechanism into future models of filament formation. Modeling of white-light propagation, however, may turn out to be difficult because of the strong dispersion of the higher-order coefficients, and methods for efficient modeling of dispersive nonlinearities may have to be found. We believe that this work has important consequences for nonlinear optics in general and in particular for nonlinear plasma optics. In fact, this may truly induce a paradigm shift in the understanding of filamentation.

Financial support by the Deutsche Forschungsgemeinschaft, grants DE 1209/1-2 and STE 762/7-2, is gratefully acknowledged. GS gratefully acknowledges support by the Academy of Finland (project grant 128844).

References

[1] A. McPherson *et al.* J. Opt. Soc. Am. B **4**, 595 (1987); X. F. Li, A. L'Huillier, M. Ferray, L. A. Lompré, and G. Mainfray, Phys. Rev. A **39**, 575 (1989).

[2] J. T. Manassah and M. A. Mustafa, Opt. Lett. **13**, 862 (1988).

[3] A. Vinçotte and L. Bergé, Phys. Rev. A **70**, 061802 (2004).

[4] S. Champeaux, L. Bergé, D. Gordon, A. Ting, J. Peñano, and P. Sprangle, Phys. Rev. E **77**, 036406 (2008).

[5] P. B. Corkum, C. Rolland, and T. Srinivasan-Rao, Phys. Rev. Lett. **57**, 2268 (1986).

[6] S. Skupin *et al.*, Phys. Rev. E **74**, 056604 (2006).

[7] A. L. Gaeta, Phys. Rev. Lett. **65**, 3582 (2000).

[8] V. Loriot, E. Hertz, O. Faucher, and B. Lavorel, Opt. Express **17**, 13429 (2009); Opt. Express **18**, 3011(E) (2010).

[9] P. Béjot, J. Kasparian, S. Henin, V. Loriot, T. Vieillard, E. Hertz, O. Faucher, B. Lavorel, and J.-P. Wolf, Phys. Rev. Lett. **104**, 103903 (2010).

[10] M. Kolesik, E. M. Wright, and J. V. Moloney, Opt. Lett. **35**, 2550 (2010).

[11] D. C. Hutchings, M. Sheik-Bahae, D. J. Hagan, and E. W. Van Stryland, Opt. Quantum Electron. **24**, 1 (1992)

[12] S. V. Popruzhenko, V. D. Mur, V. S. Popov, and D. Bauer, Phys. Rev. Lett. **101**, 193003 (2008).

[13] A. M. Perelomov, V. S. Popov, and M. V. Terent'ev, Sov. Phys. JETP **23**, 924 (1966).

[14] M. Abramowitz and I. A. Stegun (Eds.), Handbook of Mathematical Functions. 9th printing. New York: Dover, pp. 295 and 319, 1972.

[15] M. Sheik-Bahae, D. J. Hagan, and E. W. van Stryland, Phys. Rev. Lett. **65**, 96 (1990); M. Sheik-Bahae, D. C. Hutchings, D. J. Hagan, and E. W. van Stryland, IEEE J. Quantum Electron. **27**, 1296 (1991).

[16] D. M. Bishop and J. Pipin, J. Chem. Phys. **91**, 3549 (1989).

[17] H. J. Lehmeier, W. Leupacher, and A. Penzkofer, Opt. Commun. **56**, 67 (1985).

[18] C. Brée, A. Demican, and G. Steinmeyer, IEEE J. Quantum Electron. **46**, 433 (2010).

[19] D. P. Shelton and J. E. Rice, Chem. Rev. **94**, 3 (1994)

[20] J. E. Rice, J. Chem. Phys. **96**, 7580 (1992).

[21] M. Nurhuda, A. Suda, and K. Midorikawa, New J. Phys. **10**, 053006 (2008).